Dirac quantum cellular automaton in one dimension: *Zitterbewegung* and scattering from potential

Alessandro Bisio,[*] Giacomo Mauro D'Ariano,[†] and Alessandro Tosini[‡]

Dipartimento di Fisica dell'Università di Pavia and Istituto Nazionale di Fisica Nucleare, Gruppo IV, via Bassi 6, 27100 Pavia, Italy

We study the dynamical behavior of a quantum cellular automaton which reproduces the Dirac dynamics in the limit of small wave vectors and masses. We present analytical evaluations along with computer simulations, showing that the automaton exhibits typical Dirac dynamical features, such as the *Zitterbewegung* and, considering the scattering from potential, the so-called Klein paradox. The motivation is to show concretely how pure processing of quantum information can lead to particle mechanics as an emergent feature, an issue that has been the focus of solid-state, optical, and atomic-physics quantum simulators.

I. INTRODUCTION

The idea of reproducing the evolution of a macroscopic system starting from a simple rule of local interaction among its elementary constituents was first formalized in von Neumann's pioneering paper [1] with the notion of the *cellular automaton*. The automaton is a regular lattice of cells with a finite number of states, equipped with a rule that updates the cell states from time t to time $t + 1$. This rule must be *local*, namely, the state of the x cell at $t + 1$ depends only on the states of a finite number of neighboring cells at t. Cellular automata have been a popular topic for many years, as a new paradigm for complex systems, and many books have been devoted to the subject (see, e.g., Refs. [2,3]). One of the reasons for its first success, which eventually has become its own weakness, is the chaotic behavior of the automaton dynamics [4].

Differently from classical cellular automata, *quantum cellular automatons* (QCAs) exhibit a less chaotic behavior, which makes them predictable for large number of steps [5]. Here the cells are finite-dimensional quantum systems interacting locally and unitarily. Locality of interactions being an essential ingredient of any physical evolution, QCAs have been considered by Feynman as candidates for simulating physics [6,7]. More recently QCAs received interest in the quantum information community, leading to many results on their mathematical theory [8–10] and on their general dynamical features [5,11–14]. In quantum-field theory, after the first appearance of a prototype of QCA in the Feynman chessboard [6], which discretizes the Dirac-field path integral, a similar framework appeared in the work of Nakamura [15], motivated by a rigorous formulation of the Feynman path integral, and later in the seminal work of Bialynicki-Birula [16], as a lattice theory for Weyl, Dirac, and Maxwell fields. Then the possibility of using automatons for describing the evolution of relativistic fields emerged in the context of lattice-gas simulations, especially in the work of Meyer [17], where the notion of "field automaton" first appeared, and in the papers by Yepez [18].

More recently QCAs have been considered for extending quantum-field theory [19] to the Plank scale. In this context the one-dimensional Dirac automaton has been derived from the symmetries of the QCA [20] showing how the usual Dirac dynamics emerges at the Fermi scale, though relativistic covariance and other symmetries are violated at the Planck/ultrarelativistic scale. Similarly to lattice-gas theories, here the quantum cell corresponds to the evaluation $\psi(x)$ of a quantum field on site x of a lattice, with the dynamics updated in discrete time steps by a local unitary evolution. However, differently from the lattice-gas approach, here the continuum limit is not taken; instead, the asymptotic large-scale (Fermi) evolution is considered. Within this perspective the Lorentz covariance holds exactly in the relativistic limit of small momenta and masses, whereas generally it is distorted as in the deformed relativity models in Refs. [21–23].

In the present paper we analyze in detail the one-particle sector of the automaton of Refs. [19,20]. Here, particle states are "smooth" states peaked around a momentum eigenstate of the QCA. We consider dynamical quantities such as the particle position, momentum, and velocity, along with their evolution both in the free case and in the presence of a potential, recovering typical features of Dirac quantum-field evolution—such as *Zitterbewegung* and the *Klein paradox*—from the pure quantum information processing of the QCA. Recently there has been a renewed interest in Dirac features in solid-state and atomic physics, which provide the physical hardware to simulate the dynamics. *Zitterbewegung* can be seen in the response of electrons to external fields [24] and can appear for nonrelativistic particles in a crystal [25–27], quasiparticles in superconductors [28], and systems with spin-orbit coupling [29,30]. Proving that the oscillation behavior is not unique to Dirac electrons, but rather is a generic feature of spinor systems with linear dispersion relations, these works opened the way for possible simulation of *Zitterbewegung* using, for example, trapped ions [31,32], two-band crystalline structures such as graphene [33,34] and semiconductors [35–39], ultracold atoms [40], and, finally, photonic crystals [41]. On the other hand, the Klein paradox (tunneling of relativistic particles) provides insight into the mechanics of relativistic particles propagating through potential barriers and into vacuum polarization effects. Moreover, the Klein paradox has been a focus of the topic of graphene as a simulator for the Dirac equation, as in Refs. [32,42,43], and for trapped ions. Recently also microfabricated optical waveguide circuits have become an alternative physical simulator for particle dynamics [44].

---

[*]alessandro.bisio@unipv.it

[†]dariano@unipv.it

[‡]alessandro.tosini@unipv.it

After reviewing the Dirac QCA in one dimension in Sec. II, in Section III we present the evolution of position and momentum operators for the automaton, showing the *Zitterbewegung* behavior produced by the interference between positive and negative frequencies. In Sec. IV we modify the QCA in order to insert a potential in the free evolution and show the automaton dynamics in the presence of a barrier for one-particle states. We end the paper with a summary and some concluding remarks in Sec. V.

II. THE DIRAC AUTOMATON

The quantum automaton corresponding to the Dirac equation in one dimension, first introduced in [19], has been derived from the discrete automaton symmetries of parity and time-reversal in Ref. [20], where also the Dirac equation has been recovered as the large-scale relativistic limit of the automaton. The cell of the quantum automaton is given by the evaluation $\psi(x)$ of the two-component field operator ψ, and the unitary evolution of one step of the automaton is given by

$$\psi(x) \to U\psi(x), \quad \psi(x) := \begin{pmatrix} \psi_r(x) \\ \psi_l(x) \end{pmatrix}, \qquad (1)$$

where ψ_l and ψ_r denote the *left* and *right* modes of the field, respectively, whereas the unitary matrix U is given by

$$U = \begin{pmatrix} nS & -im \\ -im & nS^\dagger \end{pmatrix}, \quad n^2 + m^2 = 1, \qquad (2)$$

with S denoting the shift operator $Sf(x) = f(x+1)$. The constants n and m in Eq. (2) can be chosen positive. As shown in Refs. [19,20], the parameter m plays the role of an adimensional inertial mass and it is bounded by one. We remark that the automaton description is completely adimensional, and a conversion to the usual physical dimensions requires the length, time, and mass, which one can take as the Planck length ℓ_P, the Planck time τ_P, and the Planck mass m_P, the latter playing the role of the bound for the inertial mass. The maximal speed of propagation of information is one cell per step ($c = \ell_P/\tau_P$ in dimensional units, corresponding to the speed of light). The quantum field can be taken generally as fermionic, bosonic, or even anyonic. However, in the present case it is not relevant, since we consider only single-particle states, which span the Hilbert space $\mathbb{C}^2 \otimes l_2(\mathbb{Z})$, and for which we use the factorized orthonormal basis $|s\rangle|x\rangle$, where for $|s\rangle$ we consider the canonical basis corresponding to $s = l,r$. These states can also be obtained as $\psi_s^\dagger(x)|\Omega\rangle$ upon introducing a vacuum $|\Omega\rangle$ which is annihilated by the field operator and invariant under the automaton evolution. Similarly, also N-particle states with $N > 1$ can be obtained by acting with products of N evaluations of the field operator, building up the Fock space in the usual way. Note that the evolution of the field is restricted to be linear, and there exists a unitary operator U such that the field evolution is given by $V\psi_s(x)V^\dagger = U\psi_s(x)$, with $V|\Omega\rangle = |\Omega\rangle$, whereas for the product of field evaluations the evolution is given by tensor powers of U as $V\psi_{s_1}(x_1)\dots\psi_{s_N}(x_N)V^\dagger = U^{\otimes N}\psi_{s_1}(x_1) \otimes \dots \otimes \psi_{s_N}(x_N)$.

In the $|s\rangle|x\rangle$ representation the unitary matrix U can be written as

$$U := \sum_x \begin{pmatrix} n|x-1\rangle\langle x| & -im|x\rangle\langle x| \\ -im|x\rangle\langle x| & n|x+1\rangle\langle x| \end{pmatrix}, \qquad (3)$$

describing a *quantum walk* on the Hilbert space $\mathbb{C}^2 \otimes l_2(\mathbb{Z})$ [5].

Thanks to the translational invariance of U, it is convenient to move to the momentum representation,

$$|k\rangle := \frac{1}{\sqrt{2\pi}} \sum_x e^{-ikx}|x\rangle, \quad k \in [-\pi,\pi], \qquad (4)$$

and U becomes

$$U = \int_{-\pi}^{\pi} dk\, U(k) \otimes |k\rangle\langle k|, \quad U(k) = \begin{pmatrix} ne^{ik} & -im \\ -im & ne^{-ik} \end{pmatrix}. \qquad (5)$$

As in solid-state physics, the discreteness implies that momenta k are constrained to the Brillouin zone, namely, $|k| \leqslant \pi$. By diagonalizing the unitary matrix $U(k)$,

$$U(k)|s\rangle_k = e^{-is\omega(k)}|s\rangle_k, \quad \omega(k) = \arccos(n\cos k),$$

$$|s\rangle_k := \frac{1}{\sqrt{2}} \begin{bmatrix} \sqrt{1 - sv(k)} \\ s\sqrt{1 + sv(k)} \end{bmatrix}, \quad s = \pm, \quad v(k) := \partial_k\omega(k), \qquad (6)$$

it is easy to evaluate the logarithm of U ($e^{-iH} := U$) as

$$H = \int_{-\pi}^{\pi} dk\, H(k) \otimes |k\rangle\langle k|,$$
$$H(k) = \omega(k)\left(|+\rangle_k\langle+|_k - |-\rangle_k\langle-|_k\right)$$
$$= \operatorname{sinc}^{-1}\omega(k)(-n\sin k\,\sigma_3 + m\sigma_1), \qquad (7)$$

where σ_i $i = 1,2,3$ denote the Pauli matrices.

The function $\omega(k)$ is the dispersion relation of the automaton, which recovers the usual Dirac one $\omega(k) = \sqrt{k^2 + m^2}$ in the limit $k,m \ll 1$, as shown in [20]. This is also clear in Fig. 1, where the dispersion relation as a function of k is reported for four values of the mass. The derivative $v(k)$ in Eq. (6) is then the group velocity of the wave packet which is peaked around the wave vector k. The $s = +1$ eigenvalues correspond to positive-energy particle states, whereas the negative $s = -1$ eigenvalues correspond to negative-energy antiparticle states.
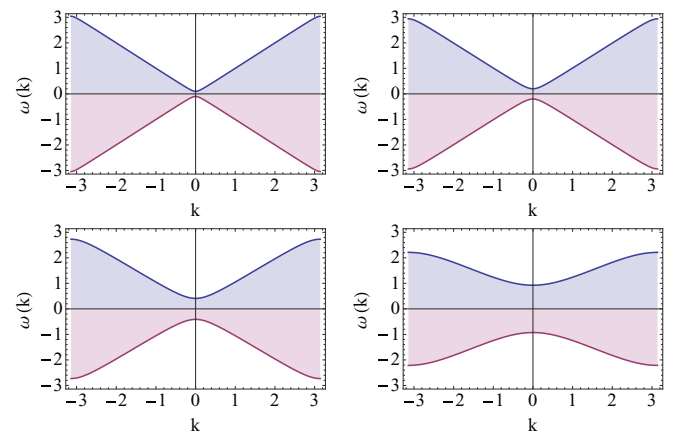

FIG. 1. (Color online) The Dirac automaton dispersion relation in Eq. (6) for four values of the mass: $m = 0.1$, 0.2, 0.4, and 0.8.

Note that the operator H, regarded as a Hamiltonian, describes the evolution for continuous times ($U(t) \equiv U^t$), which in this context has no physical meaning.

In the following sections we analyze two typical aspects of the Dirac-field dynamics, namely, *Zitterbewegung* and the Klein paradox.

III. POSITION AND MOMENTUM OPERATORS AND *ZITTERBEWEGUNG*

The QCA, (2), recovers the Dirac-field dynamics for customary relativistic wave vectors and energies (consider that, e.g., an ultrahigh-energy cosmic ray has $k \simeq 10^{-8}$) [20]. In this section we show how efficiently it reproduces a typical feature of the one-particle Dirac dynamics, namely, the *Zitterbewegung*.

The *Zitterbewegung* was first recognized in 1930 by Schrödinger [46], who noticed that in the Dirac equation describing a free relativistic electron the velocity operator does not commute with the Dirac Hamiltonian: the evolution of the position operator, in addition to the classical motion, shows a very fast periodic oscillation, with frequency $2mc^2$ and amplitude equal to the Compton wavelength $\hbar/mc$, with m the rest mass of the relativistic particle. This jittering motion first encountered in the Dirac theory of the electron was then shown [24] to arise from the interference of states corresponding to the positive and negative energies resulting from the Dirac equation, with the trembling disappearing with time [47] for a wave-packed particle state. *Zitterbewegung* oscillations cannot be directly observed by current experimental techniques for a Dirac electron since the amplitude should by very low, $\approx 10^{-12}$ m. However, it can be seen in a number of solid-state, atomic physics, photonic-crystal, and optical waveguide simulators, as stated in Sec. I.

The "position" operator X providing the representation $|x\rangle$ (i.e., such that $X|s\rangle|x\rangle = x|s\rangle|x\rangle$) is defined as follows:

$$X = \sum_{x \in \mathbb{Z}} x(I \otimes |x\rangle\langle x|). \tag{8}$$

Generally, X provides the average location of a state

$$|\psi\rangle = \sum_{\substack{x \in \mathbb{Z} \\ s = r, l}} f_s(x)|s\rangle|x\rangle \tag{9}$$

in terms of $\langle \psi | X | \psi \rangle$. If we take as the conjugated "momentum" the operator

$$P = \int_{-\pi}^{\pi} \frac{dk}{2\pi} k(I \otimes |k\rangle\langle k|), \tag{10}$$

we have the commutation relation between X and P,

$$\langle \psi | [X, P] | \psi \rangle = i - \frac{i}{2} \sum_{s = r, l} (|\hat{f}_s(\pi)|^2 + \hat{f}_s(-\pi)|^2), \tag{11}$$

where $\hat{f}(k)$ is the discrete Fourier transform of $f(x)$. Equation (11) differs from the usual canonical commutation relation $[X, P] = i$ by a boundary term. This is in agreement with the existence of perfectly localizable states on the automaton, i.e., $|\psi\rangle = |\chi\rangle|x\rangle$, for which the expectation values of the commutator vanishes. However, from now on we consider states for which the boundary term is negligible.

In the following it is convenient to work with the continuous time t interpolating exactly the discrete automaton evolution, namely, U^t. However, all numerical results are given only for discrete t, namely, for repeated applications of the automaton unitary U in Eq. (2).

The time evolution of the position operator $X(t) = U^{-t} X U^t$ can be more easily computed by integrating the differential equation $A(t) = [H, [H, X(t)]]$, where H was defined in Eq. (7). We have

$$A(t) = \int_{-\pi}^{\pi} dk \, A(k, t) \otimes |k\rangle\langle k|, \quad A(k, t) = e^{2iH(k)t} A(k),$$
$$A(k) = -\frac{2\omega^2}{\sin^2 \omega} nm \cos k \, \sigma_2, \tag{12}$$

which leads to

$$X(t) = X(0) + Vt + Z_X(t) - Z_X(0), \tag{13}$$

$$V(k) = -v(k)^2 \sigma_3 + v(k)\sqrt{1 - v(k)^2} \sigma_1, \tag{14}$$

$$Z_X(k, t) = -\tfrac{1}{4} H^{-2}(k) A(k, t), \tag{15}$$

where V is the classical component of the velocity operator, which, in the base diagonalizing Hamiltonian (7), is $V(k) = v(k)\sigma_3$ and is proportional to the group velocity $v(k)$. Since the generic one-particle state $|\psi\rangle$ is the superposition of a positive and a negative energy state, i.e., $|\psi_+\rangle + |\psi_-\rangle$, the evolution of the mean value of the position operator, $X(t)$, can be written as

$$x_\psi(t) := \langle \psi | X(t) | \psi \rangle = x_\psi^+(t) + x_\psi^-(t) + x_\psi^{\text{int}}(t),$$
$$x_\psi^{\pm}(t) := \langle \psi_\pm | X(0) + Vt | \psi_\pm \rangle, \tag{16}$$
$$x_\psi^{\text{int}}(t) := 2\text{Re}[\langle \psi_+ | X(0) - Z_X(0) + Z_X(t) | \psi_- \rangle],$$

where Re denotes the real part. The interference between positive and negative frequency is responsible for the oscillating term $x_\psi^{\text{int}}(t)$ whose magnitude is bounded by $1/m$ (see the Appendix), which, in the usual dimensional units, corresponds to the Compton wavelength $\hbar/mc$. These results show that $x_\psi^{\text{int}}(t)$ is the automaton analog of the so-called *Zitterbewegung*. In the Appendix we show that for $t \to \infty$ the term $2\text{Re}[\langle \psi_+ | Z_X(t) | \psi_- \rangle]$, which is responsible for the oscillation, goes to 0 as $1/\sqrt{t}$, and only the shift contribution coming from $2\text{Re}[\langle \psi_+ | X(0) - Z_X(0) | \psi_- \rangle]$ survives. Note that this asymptotic behavior could be different in the presence of a potential as shown in Refs. [49,50], where a revival of *Zitterbewegung* occurs for a Dirac oscillator. As noted in Sec. I, this phenomenon was never observed for a free relativistic electron because of the small value of the electron Compton wavelength, which is 10^{-12} m. The results in this section are in agreement with those for the Hadamard walk [51].

In Fig. 3 we have considered the evolution of states with particle and antiparticle components smoothly peaked around some momentum eigenstate, namely,

$$c_+|\psi_+\rangle + c_-|\psi_-\rangle, \quad |\psi_\pm\rangle = \int \frac{dk}{\sqrt{2\pi}} g_{k_0}(k)|\pm\rangle_k|k\rangle, \tag{17}$$

where $|c_+|^2 + |c_-|^2 = 1$ and g_{k_0} is a Gaussian peaked around the momentum k_0 with width σ. An easy computation shows that for these states the shift
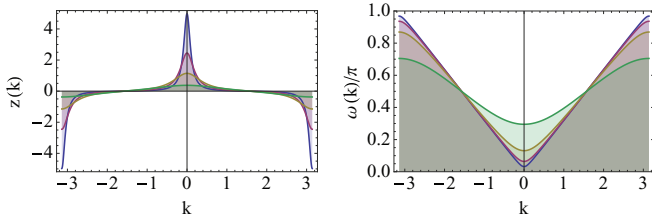
FIG. 2. (Color online) Plots of $z(k)$ (left) and $\omega(k)/\pi$ (right) related to the oscillation amplitude and frequency of the position expectation value in Eq. (13). In both cases the plots are reported for different values of the mass ($m = 0.1, 0.2, 0.4,$ and 0.8, from top to bottom (left) and from bottom to top (right).

contribution reduces to $2\text{Re}[\langle\psi|X(0) + Z_X(0)|\psi\rangle] = \text{Im}(c_+^* c_-)/(2\pi)\int_{-\pi}^{\pi} dk\,|g_{k_0}(k)|^2 z(k)$, with the function $z(k) = m\cos\omega(k)/\sin^2\omega(k)$ bounded again by the Compton wavelength $1/m$ and the oscillation frequency given by $\omega(0)/\pi$ (see also Fig. 2). It is worth noting that when the wave packets are both peaked around $k = 0$, as in the first two cases in Fig. 3, the damping of the oscillation amplitude can be observed for times much longer than those we could consider in our simulation. Indeed, since the wave packet is sharp in $k = 0$, the asymptotic approximation of Eq. (A1) proves to be accurate only for very large values of t.

IV. EVOLUTION WITH A SQUARE POTENTIAL BARRIER

In order to study the scattering with a potential, we modify the automaton, adding a position-dependent phase representing a square potential barrier, as in Refs. [51,52]. We provide explicitly the transmission T and reflection R coefficients as functions of the energy and mass of the incident wave packet and of the potential barrier's height. We find a general behavior independent of the regime, namely, of the energy and mass of the incident particle. When the value of the potential barrier is increased beyond a certain threshold the transmitted wave reappears and the reflection coefficient starts to decrease. The width of the $R = 1$ region is an increasing function of the mass, which is proportional to the gap between positive- and negative-frequency eigenvalues of the unitary evolution.

For a generic potential $\phi(x)$, the unitary evolution becomes

$$U_\phi := \sum_x e^{-i\phi(x)}\begin{pmatrix} n|x-1\rangle\langle x| & -im|x\rangle\langle x| \\ -im|x\rangle\langle x| & n|x+1\rangle\langle x| \end{pmatrix}.$$

We analyze the simple case $\phi(x) := \phi\,\theta(x)$ [$\theta(x)$ is the Heaviside step function], which is a potential step that is 0 for $x < 0$ (region I) and has a constant value $\phi \in [0,2\pi]$ for $x \geqslant 0$ (region II) as illustrated in Fig. 4.

Let us now study the eigenvector of U_ϕ of the form

$$|\Phi_k\rangle = \Pi_I|+\rangle_k|k\rangle + \Pi_I\beta_k|+\rangle_{-k}|k\rangle + \gamma_k\Pi_{II}|+\rangle_{k'}|k'\rangle,$$

$$\Pi_I := \sum_{x<0} I\otimes|x\rangle\langle x|, \quad \Pi_{II} := \sum_{x\geqslant 0} I\otimes|x\rangle\langle x|,$$
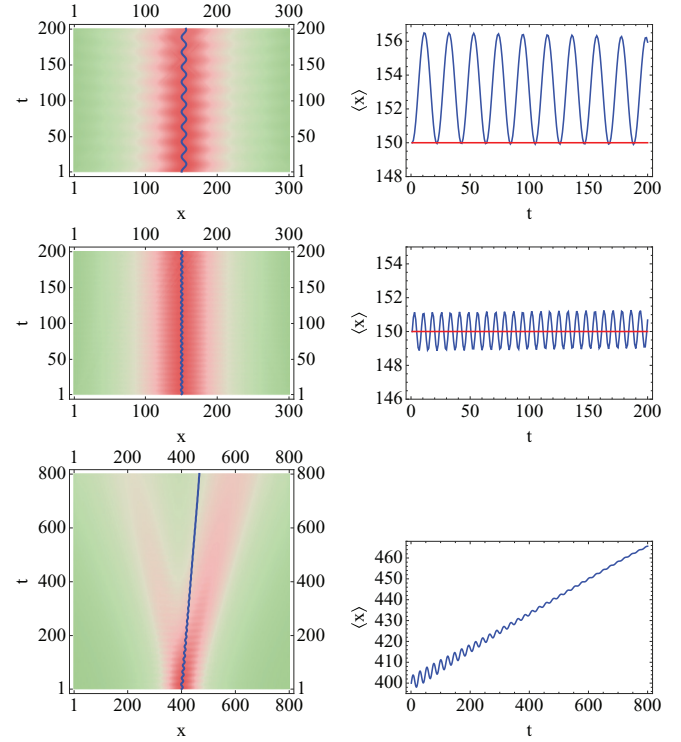

FIG. 3. (Color online) Automaton evolution of a state as in Eq. (17) showing the *Zitterbewegung* of the position expectation value. Top: $m = 0.15$, $c_+ = 1/\sqrt{2}$, $c_- = i/\sqrt{2}$, $k_0 = 0$, and $\sigma = 40^{-1}$. The calculated shift and oscillation frequency are, respectively, $\langle\psi|X(0) + Z_X(0)|\psi\rangle = 3.2$ and $\omega(0)/\pi = 0.05$, according to the simulation. Middle: $m = 0.15$, $c_+ = 1/\sqrt{2}$, $c_- = 1/\sqrt{2}$, $k_0 = 0$, $\sigma = 40^{-1}$. The calculated shift and oscillation frequency are 0 and 0.13, respectively. Bottom: $m = 0.13$, $c_+ = \sqrt{2/3}$, $c_- = 1/\sqrt{3}$, $k_0 = 10^{-2}\pi$, $\sigma = 40^{-1}$. In this case the particle and antiparticle contribution are not balanced and the average position drift velocity is thus $\langle\psi_+|V|\psi_+\rangle + \langle\psi_-|V|\psi_-\rangle = (|c_+|^2 - |c_-|^2)v(k_0) = 0.08$, corresponding to an average position $x_\psi^+(800) + x_\psi^-(800) = 464$ [see Eq. (16)]. Note that for $t \to \infty$ the term $2\text{Re}[\langle\psi_+|Z_X(t)|\psi_-\rangle$, which is responsible for the oscillation, goes to 0.

where β_k, γ_k, and k' are functions of k. The condition that $|\Phi_k\rangle$ is an eigenstate of U_ϕ, i.e., $U_\phi|\Phi_k\rangle = e^{-i\omega(k)}|\Phi_k\rangle$, implies that
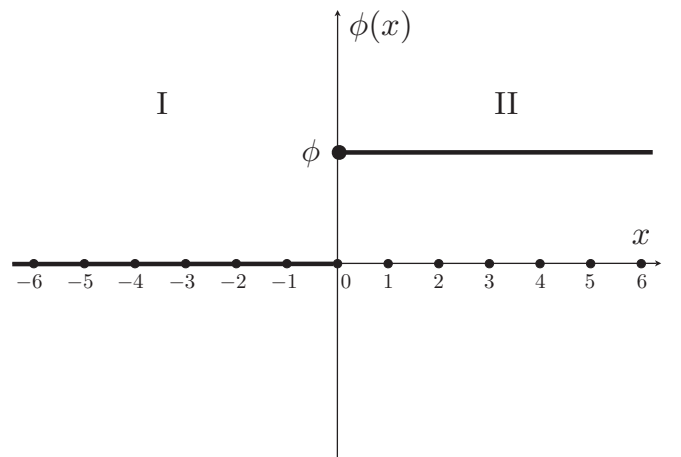

FIG. 4. Schematic of the potential.

$$\omega(k') = \omega(k) - \phi,$$

$$\beta_k = \frac{e^{-ik}\sqrt{(1+v)(1-v')} - e^{-ik'}\sqrt{(1-v)(1+v')}}{-e^{ik}\sqrt{(1-v)(1-v')} + e^{-ik'}\sqrt{(1+v)(1+v')}},$$

$$\gamma_k = \frac{2e^{i\xi}(v\cos k - i\sin k)}{-e^{ik}\sqrt{(1-v)(1-v')} + e^{-ik'}\sqrt{(1+v)(1+v')}},$$

$$(18)$$

with $v := v(k)$ and $v' := v(k')$ the group velocities of the incident and transmitted wave. Let us now consider the superposition

$$|\Psi(0)\rangle := \int \frac{dk}{\sqrt{2\pi}} g_{k_0}(k)|\Phi_k\rangle,$$

where $g_{k_0}(k)$ is a function in $C_0^\infty[-\pi,\pi]$ which we assume to be smoothly peaked around k_0. The state at time t is then

$$|\Psi(t)\rangle := \int \frac{dk}{\sqrt{2\pi}} g_{k_0}(k)e^{-i\omega(k)t}|\Phi_k\rangle,$$

and one can verify that for $t \ll 0$ the state is negligible in region II, while the only appreciable contribution in region II comes from the term $e^{ik_0 x}$, which describes a wave packet that moves at group velocity $v(k_0)$ and hits the barrier from the left. When $t \gg 0$ the state can be approximated by a superposition of the reflected and a transmitted wavepacket as

$$|\Psi(t)\rangle \xrightarrow{t \gg 0} \beta(k_0) \int \frac{dk}{\sqrt{2\pi}} g_{k_0}(k)e^{-i\omega(k)t}|+\rangle_{-k}|k\rangle$$

$$+ \tilde{\gamma}(k_0)e^{-i\phi t} \int \frac{dk}{\sqrt{2\pi}} \tilde{g}_{k_0'}(k')e^{-i\omega(k')t}|+\rangle_{k'}|k'\rangle,$$

where we have defined

$$k_0' \text{ s.t. } \omega(k_0') = \omega(k_0) - \phi,$$

$$\tilde{\gamma}(k_0) := \gamma(k_0)\sqrt{\frac{v(k_0')}{v(k_0)}},$$

$$\tilde{g}_{k_0'}(k') = \sqrt{\frac{v(k_0')}{v(k_0)}} g_{k_0'}(k')$$

(one can check $\int dk|\sqrt{2\pi}|\tilde{g}_{k_0'}(k')|^2 = 2\pi$), whose group velocities are $-v(k_0)$ for the reflected wave packet and $v(k_0')$ for the transmitted wave packet (see Fig. 5).

The probability of finding the particle in the reflected wave packet is $R = |\beta(k_0)|^2$ (reflection coefficient), while the probability of finding the particle in the transmitted wave packet is $T = |\tilde{\gamma}(k_0)|^2$ (transmission coefficient). The consistency of the result can be verified by checking that $R + T = 1$. For $k \ll m \ll 1$ (Schröedinger regime) we recover the usual reflection and transmission coefficient for the Schröedinger equation with a potential step. In Fig. 6 we plot the reflection coefficient R as a function of ϕ and k for different values of the mass m. Clearly when $\phi = 0$ we have $R = 0$ and increasing ϕ while fixing k the value increases up to $R = 1$. One may note that when $\omega(k) - \arccos(n) < \phi < \omega(k) + \arccos(n)$ Eq. (18) has a solution for imaginary k' which implies an exponential damping of the transmitted wave and pure reflection. By further increasing the value of ϕ beyond the threshold $\omega(k) + \arccos(n)$, Eq. (18) has a solution for real k' and negative $\omega(k')$, and then the transmitted wave reappears
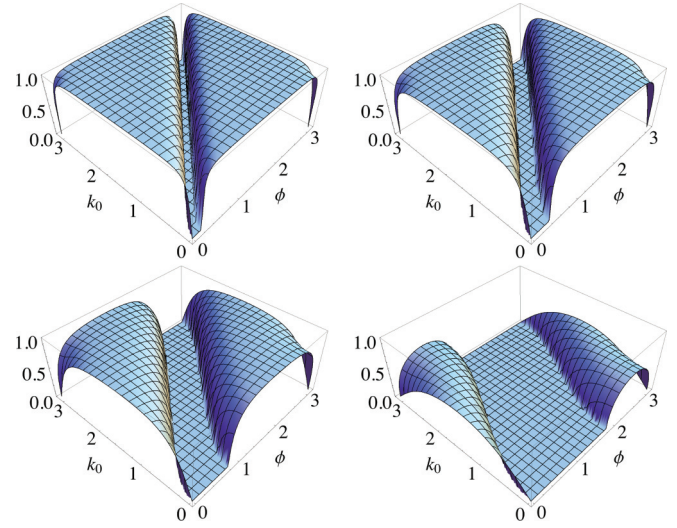

FIG. 5. (Color online) Group velocity of the transmitted wave packet as a function of the potential barrier height ϕ and of the momentum k of the incident particle state. From top left to bottom right the transmitted group velocity is depicted for values of the mass $m = 0.1, 0.2, 0.4,$ and 0.8.

and the reflection coefficient decreases. This is the so-called "Klein paradox," which is caused by the presence of positive- and negative-frequency eigenvalues of the unitary evolution. The width of the $R = 1$ region is an increasing function of the mass equal to $2\arccos(n)$, which is the gap between positive- and negative-frequency solutions (see Fig. 1).

In Fig. 7 we plot the reflection R coefficient and the transmitted wave velocity group $v(k_0')$ as a function of the potential barrier height ϕ, with the incident wave packet having $k_0 = 2$ and $m = 0.4$. From the figure it is clear that after a plateau with $R = 1$ the reflection coefficient starts decreasing for higher potentials. In Fig. 8 we show the scattering simulation for four increasing values of the potential,
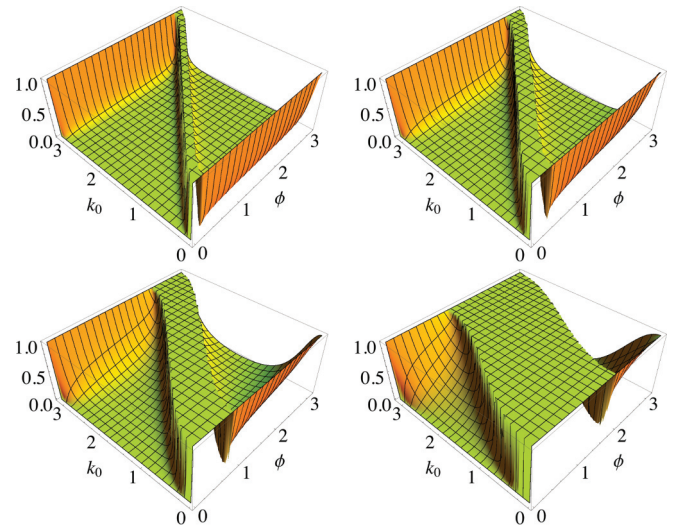

FIG. 6. (Color online) Reflection coefficient as a function of the potential barrier height ϕ and of the momentum k of the incident particle state. From top left to bottom right the reflection coefficient is depicted for values of the mass $m = 0.1, 0.2, 0.4,$ and 0.8.
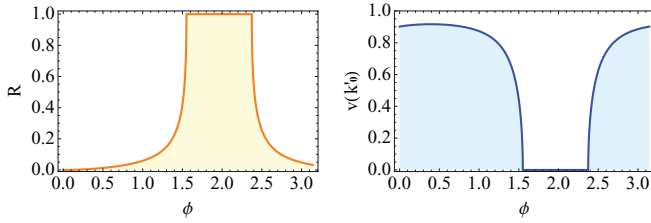
FIG. 7. (Color online) Reflection coefficient for $m = 0.4$ and momentum of the incident particle $k_0 = 2$ as a function of the potential barrier height ϕ (section of plots in Figs. 5 and 6 for $m = 0.4$, $k_0 = 2$).

say $\phi = 1.42$, 1.55, 2, and 2.4 (see the figure caption for details).

V. CONCLUSIONS

In this paper we have studied the dynamics of the QCA in Refs. [19,20], which gives the Dirac dynamics as emergent in the limit of small wave vectors. We have presented computer simulations and analytical evaluations, focusing on typical features of the Dirac dynamics, in particular, *Zitterbewegung* and the scattering from potential. Our automaton covers all regimes of masses and energy momenta, beyond the same validity range of the Dirac equation, with the possibility of considering arbitrary input states, enabling us to investigate and visualize a wide range of fundamental processes. These facts, in addition to the discreteness of the automaton, make it the ideal theoretical counterpart for the experimental simulators in the literature. A similar quantum cellular automaton
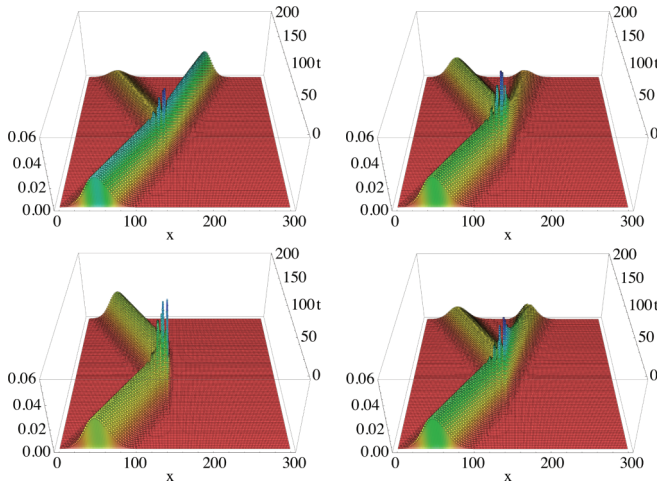

FIG. 8. (Color online) Simulations of the Dirac automaton evolution with a square potential barrier. Here the automaton mass is $m = 0.2$, while the barrier turns on at $x = 140$. In the simulation the incident state is a smooth state of the form $|\psi(0)\rangle = \int dk \sqrt{2\pi} g_{k_0}(k) |+\rangle_k$ peaked around the positive energy eigenstate $|+\rangle_{k_0}$ with $k_0 = 2$ and with g_{k_0} a Gaussian having width $\sigma = 15^{-1}$. The incident group velocity is $v(k_0) = 0.90$. The simulation is run for four increasing values of the potential ϕ. Top left: Potential barrier height $\phi = 1.42$, reflection coefficient $R = 0.25$, velocity of the transmitted particle $v(k'_0) = 0.63$. Top right: $\phi = 1.55$, $R = 0.75$, $v(k'_0) = 0.1$. Bottom left: $\phi = 2$, $R = 0.1$, $v(k'_0) = 0$. Bottom right: $\phi = 2.4$, $R = 0.50$, $v(k'_0) = 0.33$.

can also be developed in two dimensions [53], corresponding to graphene as a quantum simulator.

APPENDIX: BOUND OF THE OSCILLATING TERM AND ITS ASYMPTOTIC BEHAVIOR

Here we provide an upper bound for the oscillating term $x_\psi^{\mathrm{int}}(t)$ in Eq. (16) in the position operator evolution derived in Sec. III and we derive its behavior for very long time steps. The jittering of the position expectation value is caused by the operator $Z_X(t)$ which in the base diagonalizing the automaton Hamiltonian H (7) can be written as

$$Z_X(t) = \int_{-\pi}^{\pi} dk\, e^{2i\omega(k)\sigma_z t} Z_X(k) \otimes |k\rangle\langle k|,$$

$$Z_X(k) = z(k)\sigma_2, \quad z(k) = \frac{m\cos\omega(k)}{2\sin^2\omega(k)},$$

with $z(k) \in L^1(-\pi,\pi)$ for any $m \neq 0$. By defining

$$|\psi_\pm\rangle = \int_{-\pi}^{\pi} \frac{dk}{\sqrt{2\pi}} g_\pm(k)|\pm\rangle_k |k\rangle, \quad g_\pm(k) \in C_0^\infty[-\pi,\pi],$$

we have

$$2\mathrm{Re}[\langle\psi_+|Z_X(t)|\psi_-\rangle] = \int_{-\pi}^{\pi} \frac{dk}{\pi} z(k)\mathrm{Re}[i g_+^*(k) g_-(k) e^{2i\omega(k)t}].$$

Since, for any $m \neq 0$, $\omega(k)$ has three stationary points in $k = 0, \pm\pi$ [$\omega^{(1)}(0) = \omega^{(1)}(\pm\pi) = 0$ and $\omega^{(1)}(k) \neq 0$ elsewhere in the closed interval $k \in [-\pi,\pi]$, with $\omega^{(2)}(0), \omega^{(2)}(\pm\pi) \neq 0$], the stationary phase approximation gives

$$2\mathrm{Re}[\langle\psi_+|Z_X(t)|\psi_-\rangle]$$
$$\xrightarrow{t \gg 0} \sum_{k=0,\pm\pi} z(k)\mathrm{Re}\left[i g_+^*(k) g_-(k) e^{2i\omega(k)t} \sqrt{\frac{i}{\pi\omega^{(2)}(k)t}}\right],$$
$$\tag{A1}$$

showing that the term $2\mathrm{Re}[\langle\psi_+|Z_X(t)|\psi_-\rangle]$ goes to 0 as $1/\sqrt{t}$.

In order to find an upper bound for $x_\psi^{\mathrm{int}}(t)$ note that

$$\left|x_\psi^{\mathrm{int}}(t)\right| \leqslant 2|\langle\psi_+|X(0) - Z_X(0) + Z_X(t)|\psi_-\rangle|$$
$$\leqslant 2(|\langle\psi_+|X(0)|\psi_-\rangle| + |Z_X(0)| + |Z_X(t)|),$$

and according to the expression of $Z_X(k)$, we get

$$|Z_X(0)| + |Z_X(t)| \leqslant 2|Z_X(0)|,$$

$$|Z_X(0)| \leqslant \max_{k \in [-\pi,\pi]} |z(k)| = z(0) = \frac{\sqrt{1-m^2}}{2m}.$$

Now defining the $C_0^\infty[-\pi,\pi]$ test function $\varphi(k,k') = g_+^*(k)g_-(k')\langle+|_k|-\rangle_{k'}$, we have

$$|\langle\psi_+|X(0)|\psi_-\rangle| = \left|\left\langle\frac{d\delta(k-k')}{d(k-k')}\middle|\varphi(k,k')\right\rangle\right| = \left|\left\langle\delta(k-k')\middle|\frac{d\varphi(k,k')}{d(k-k')}\right\rangle\right|$$

$$= \left|\int_{-\pi}^{\pi}\frac{dk}{2\pi}\,dk'\,\delta(k-k')g_+^*(k)g_-(k')\frac{d}{d(k-k')}\langle+|_k|-\rangle_{k'}\right|$$

$$= \left|\int_{-\pi}^{\pi}\frac{dk}{2\pi}g_+^*(k)g_-(k)f(k)\right| \leqslant \max_{k\in[-\pi,\pi]}|f(k)| = f(0),$$

$$f(k) := \frac{n}{\sin^2\omega}, \quad f(0) = \frac{\sqrt{1-m^2}}{m^2},$$

which, finally, gives

$$\left|x_\psi^{\text{int}}(t)\right| \leqslant \frac{2}{m} + \frac{2}{m^2}. \tag{A2}$$

[1] J. von Neumann, *Theory of Self-reproducing Automata* (University of Illinois Press, Urbana, 1966).

[2] S. Wolfram, *A New Kind of Science* (Wolfram Media, Champaign, IL, 2002), Vol. 5.

[3] T. Toffoli and N. Margolus, *Cellular Automata Machines* (MIT Press, Cambridge, MA, 1987).

[4] F. Berto and J. Tagliabue, in *The Stanford Encyclopedia of Philosophy*, summer 2012 ed., edited by E. N. Zalta (plato.stanford.edu, 2012).

[5] A. Ambainis, E. Bach, A. Nayak, A. Vishwanath, and J. Watrous, in *Proceedings of the Thirty-third Annual ACM Symposium on Theory of Computing* (ACM Press, New York, 2001), pp. 37–49.

[6] R. P. Feynman, A. R. Hibbs, and D. F. Styer, *Quantum Mechanics and Path Integrals, Vol. 2* (McGraw–Hill, New York, 1965).

[7] R. Feynman, Int. J. Theor. Phys. **21**, 467 (1982).

[8] B. Schumacher and R. Werner, arXiv:quant-ph/0405174.

[9] P. Arrighi, V. Nesme, and R. Werner, J. Comput. Syst. Sci. **77**, 372 (2011).

[10] D. Gross, V. Nesme, H. Vogts, and R. Werner, Commun. Math. Phys. **310**, 419 (2012).

[11] P. Knight, E. Roldán, and J. Sipe, J. Mod. Opt. **51**, 1761 (2004).

[12] G. Valcárcel, E. Roldán, and A. Romanelli, New J. Phys. **12**, 123022 (2010).

[13] A. Ahlbrecht, H. Vogts, A. Werner, and R. Werner, J. Math. Phys. **52**, 042201 (2011).

[14] D. Reitzner, D. Nagaj, and V. Bužek, Acta Phys. Slov. Rev. Tutor. **61**, 603 (2011).

[15] T. Nakamura, J. Math. Phys. **32**, 457 (1991).

[16] I. Bialynicki-Birula, Phys. Rev. D **49**, 6920 (1994).

[17] D. Meyer, J. Stat. Phys. **85**, 551 (1996).

[18] J. Yepez, Quantum Inform. Process. **4**, 471 (2006).

[19] G. M. D'Ariano, Phys. Lett. A **376** (2011).

[20] A. Bisio, G. D'Ariano, and A. Tosini, arXiv:1212.2839.

[21] J. Magueijo and L. Smolin, Phys. Rev. D **67**, 044017 (2003).

[22] Amelino-Camelia, Int. J. Modern Phys. D **11**, 35 (2002).

[23] G. Amelino-Camelia and T. Piran, Phys. Rev. D **64**, 036005 (2001).

[24] K. Huang, Am. J. Phys. **20**, 479 (1952).

[25] F. Cannata and L. Ferrari, Phys. Rev. B **44**, 8599 (1991).

[26] L. Ferrari and G. Russo, Phys. Rev. B **42**, 7454 (1990).

[27] F. Cannata, L. Ferrari, and G. Russo, Solid State Commun. **74**, 309 (1990).

[28] D. Lurié and S. Cremer, Physica **50**, 224 (1970).

[29] S.-Q. Shen, Phys. Rev. Lett. **95**, 187203 (2005).

[30] E. Bernardes, J. Schliemann, M. Lee, J. C. Egues, and D. Loss, Phys. Rev. Lett. **99**, 076603 (2007).

[31] L. Lamata, J. León, T. Schätz, and E. Solano, Phys. Rev. lett. **98**, 253005 (2007).

[32] R. Gerritsma, G. Kirchmair, F. Zähringer, E. Solano, R. Blatt, and C. Roos, Nature **463**, 68 (2010).

[33] J. Cserti and G. Dávid, Phys. Rev. B **74**, 172305 (2006).

[34] T. M. Rusin and W. Zawadzki, Phys. Rev. B **76**, 195439 (2007).

[35] J. Schliemann, D. Loss, and R. M. Westervelt, Phys. Rev. Lett. **94**, 206801 (2005).

[36] W. Zawadzki, Phys. Rev. B **72**, 085217 (2005).

[37] W. Zawadzki and T. Rusin, Phys. Lett. A **374**, 3533 (2010).

[38] A. Geim and K. Novoselov, Nat. Mater. **6**, 183 (2007).

[39] W. Zawadzki and T. Rusin, J. Phys.: Condens. Matter **23**, 143201 (2011).

[40] J. Y. Vaishnav and C. W. Clark, Phys. Rev. lett. **100**, 153002 (2008).

[41] X. Zhang, Phys. Rev. Lett. **100**, 113903 (2008).

[42] M. Katsnelson, K. Novoselov, and A. Geim, Nat. Phys. **2**, 620 (2006).

[43] M. I. Katsnelson and K. Novoselov, Solid State Commun. **143**, 3 (2007).

[44] L. Sansoni, F. Sciarrino, G. Vallone, P. Mataloni, A. Crespi, R. Ramponi, and R. Osellame, Phys. Rev. Lett. **108**, 010502 (2012).

[45] The interactions described by the Hamiltonian *H* would be nonlocal since it involves an infinite number of cells.

[46] E. Schrödinger, *Über die kräftefreie Bewegung in der relativistischen Quantenmechanik* (Akademie der wissenschaften in kommission bei W. de Gruyter u. Company, 1930).

[47] J. A. Lock, Am. J. Phys **47**, I979 (1979).

[48] The true mechanical definition of momentum would require an interacting theory allowing momentum exchange between different particles.

[49] E. Romera and F. de los Santos, Phys. Rev. B **80**, 165416 (2009).

[50] E. Romera, Phys. Rev. A **84**, 052102 (2011).

[51] P. Kurzyński, Phys. Lett. A **372**, 6125 (2008).

[52] D. A. Meyer, Int. J. Mod. Phys. C **8**, 717 (1997).

[53] G. M. D'Ariano and P. Perinotti, arXiv:1306.1934.